

# SOOT YIELD OF TURBULENT PREMIXED PROPANE-OXYGEN-INERT GAS FLAMES IN A CONSTANT-VOLUME COMBUSTOR AT HIGH PRESSURES

M. W. BAE<sup>1)\*</sup>, C. W. BAE<sup>2)</sup>, S. K. LEE<sup>3)</sup> and S. W. AHN<sup>1)</sup>

<sup>1)</sup>Engineering Research Institute, School of Mechanical and Aerospace Engineering,  
Gyeongsang National University, Gyeongnam 660-701, Korea

<sup>2)</sup>Graduate School of Science and Engineering, Tokyo Institute of Technology, Yokohama 226-8503, Japan

<sup>3)</sup>School of Agricultural Systems Engineering, Gyeongsang National University, Gyeongnam 660-701, Korea

(Received 27 December 2004; Revised 21 February 2006)

**ABSTRACT**—The soot yield has been studied by a premixed propane-oxygen-inert gas combustion in a specially designed disk-type constant-volume combustion chamber to investigate the effect of pressure, temperature and turbulence on soot formation. Premixtures are simultaneously ignited by eight spark plugs located on the circumference of chamber at 45 degrees intervals in order to observe the soot formation under high temperature and high pressure. The eight converged flames compress the end gases to a high pressure. The laser schlieren and direct flame photographs with observation area of 10 mm in diameter are taken to examine the behaviors of flame front and gas flow in laminar and turbulent combustion. The soot volume fraction in the chamber center during the final stage of combustion at the highest pressure is measured by the in-situ laser extinction technique and simultaneously the corresponding burnt gas temperature by the two-color pyrometry method. The changes of pressure and temperature during soot formation are controlled by varying the initial charging pressure and the volume fraction of inert gas compositions, respectively. It is found that the soot yield increases with dropping the temperature and raising the pressure at a constant equivalence ratio, and the soot yield in turbulent combustion decreases as compared with that in laminar combustion because the burnt gas temperature increases with the drop of heat loss for laminar combustion.

**KEY WORDS** : Turbulent combustion, Soot yield, Premixed flame, High pressure, Constant-volume combustion chamber, Laser extinction technique

## 1. INTRODUCTION

Carbonaceous particulate (hereafter soot) emitted from practical combustion systems such as diesel engines, gas turbines, steam power plants, etc. is well known as one of the major air pollutants and thus reduction measures are strongly required. Even though the soot formation in the combustion system is not much elucidated yet, the following sequences have been found to be involved in soot formation: (1) fuel sprayed in the combustor became to high temperature due to heat transfer and mixing resulting from convection and radiation which are caused by high-temperature burnt gas; (2) the resultant high-temperature fuel undergoes pyrolysis process to form unsaturated, lighter hydrocarbons such as  $C_2H_2$  and  $C_2H_4$ ; (3) and finally these compounds turn into polycyclic aromatic hydrocarbons by polymerization and condensation at the same time that dehydrogenization occurs,

thereby resulting in heavier-molecular (molecular weight  $=10^6$ ) soot particulate (Kim *et al.*, 2005).

There have been many research efforts on the kinetic mechanism of nucleation and surface growth for particles, and several models have been proposed on the process of soot formation (Kennedy, 1997; Kazakov and Frenklach, 1998). As a perfect kinetic model on soot formation is not constructed yet, studies have focused on experiments with conditions for soot formation and soot yield in order to understand comprehensively the various phenomena of soot particles (Bae, 1989). Since soot formation conditions and soot yield are functions of fuels, equivalence ratio, pressure, temperature and time, determining the functional relation by representative flames and high-temperature regions will be not only useful for making up countermeasures to reduce soot emissions in practical combustion devices but also will provide comprehensive data on the above-mentioned kinetic research.

Since diffusion flames are produced in diesel engines and gas turbines, Lagrangian follow-up of a specific mix-

\*Corresponding author. e-mail: mwbae@nongae.gsnu.ac.kr

ed cluster will find that its equivalence ratio varies momentarily due to diffusion and that temperatures also vary from hour to hour due to combustion and heat transfer. The fact that the turbulence and molecular diffusions control the temporal equivalence ratio and temperature in a mixture makes it difficult to gain a general understanding of soot formation and oxidation process. In addition, although practical combustion engines form soot under high pressures, most studies have focused on a steady-flow burner combustion that produces soot at and below the atmospheric pressure, which has not made much contribution to understanding of actual phenomena.

In this study, a special constant-volume combustor was manufactured to facilitate an observation of soot formation process in premixed combustion simply with the exception of diffusion process and to measure soot concentration at high temperatures and pressures. Hopefully, the obtained data will serve as basic data on soot formation in combustion engines and will be utilized for further studies on simultaneous measurement of soot concentration and particle size. This combustor was experimentally applied to investigate the effects of pressure, temperature and turbulence on soot formation in a premixed propane-oxygen-inert gas flame, with temperature and pressure as parameters.

## 2. EXPERIMENTAL APPARATUS AND APPROACH

### 2.1. Experimental Apparatus

The combustor manufactured for this study was a disk-type, 100 mm in diameter and 14 mm in height. Installed around the combustor were eight spark plugs at intervals of 45 degrees. Refer to the authors' literature for further information (Kamimoto *et al.*, 1989).

Figure 1 presents an optical data acquisition system that measures the extents of transmitted light and self-emission intensities at two wavelengths. He-Ne laser (wavelength=632.8 nm and output=1 mW) was employed as a light source. In order to separate the laser's transmitted light intensity and self-emission intensity from soot particles, a laser beam was projected by the Bragg cell (frequency 1 kHz) into flames in a periodic, intermittent fashion. As shown in the figure, the laser beam was enlarged in diameter in advance so as to measure efficiently variations of average soot concentration in the central area of the combustion chamber. An attempt was made to project directly the laser beam alone, but the amplified laser was adopted instead, because the transmitted light measurements of both methods were almost identical. The combustor was installed to minimize the buoyancy effect.

The beam from the Bragg cell was enlarged by two

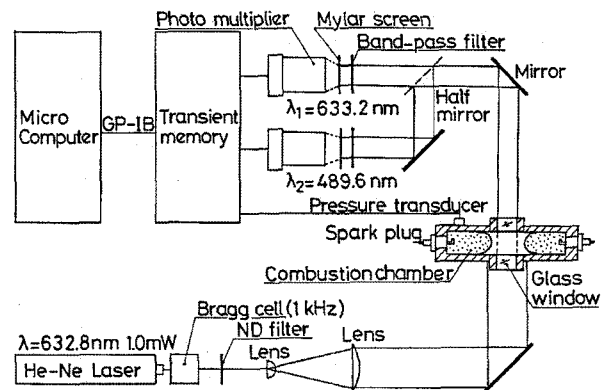


Figure 1. Schematic diagram of the experimental arrangement.

convex lenses into a parallel beam 20 mm in diameter so that the beam may fit into the observation window of 10 mm in diameter. The resultant beam was reflected at right angle by a mirror before traveling into the combustion chamber through the observation window. After being reflected at right angle by another mirror on the opposite side of the combustion chamber, the transmitted light and self-emission (effective wavelength  $\lambda_1=633.2$  nm, FWHM 3 nm), and self-emission (effective wavelength  $\lambda_2=489.6$  nm, FWHM 2.5 nm) from soot particles were passed through band-pass filters before reaching the mylar screen, and the intensities of both lights were detected by photo-multipliers respectively. The outputs from the pressure transducer and photomultipliers were acquired and stored with an on-line digital storage oscilloscope (8 bits, 4000 words) and wave memory (8 bits, 8192 words) equipped with an A/D converter, and were verified before being transmitted to a microcomputer for obtaining the pressure, burnt gas temperature, soot volume fraction and soot yield.

### 2.2. Techniques

When the wavelength of light  $\lambda$  is projected into soot particle clouds suspended irregularly in flames, the relation of transmissivity  $\tau$  to soot volume fraction  $f_v$  is defined as follows by Lambert-Beer's law and Rayleigh's equation (Bae, 1989):

$$\tau = \exp[6\pi l / \lambda \{m^2 - 1\} / (m^2 + 2)] \cdot f_v \quad (1)$$

where  $l$  is a path length of particle, and complex refractive index is represented as  $m$ , which was adopted from Dalzell & Sarofim's (1969) value.

The soot volume fraction  $f_v$  itself cannot be applied to analyze the extent of soot formation, because in this study fuel amounts included in mixtures were dependent upon the initial pressure of charged mixtures. This is why the extents of soot formation were instead evaluated by defining as soot yield  $C_s$  (%), the percentage of the

carbon that has been transformed into soot to the carbon in fuel. The relation between  $C_s$  and  $f_v$  is as follows when the normal paraffin fuels,  $C_nH_{2n+2}$ , is used.

$$C_s = \frac{7n+1}{6n} \cdot \left(1 + \frac{1}{\phi f_{st}}\right) \cdot \left(\frac{1}{1-DRm}\right) \cdot \frac{\rho_s}{\rho_{bg}} \cdot f_v \quad (2)$$

where  $n$  refers to the number of carbon atoms in fuel molecules;  $\phi$ , the equivalence ratio of mixture;  $f_{st}$ , the theoretical ratio of fuel to oxygen;  $DRm$ , the volume ratio of the inert gas to the mixtures;  $\rho_s$ , the density of the soot particles ( $1.8 \text{ g/cm}^3$ ) (Park and Appleton, 1973); and finally  $\rho_{bg}$ , the density of burnt gas at the observation area where  $f_v$  is measured.

Self-emission by flames is inevitably included in the light intensity equivalent to the laser wavelength itself that passes through the band-pass filter and is detected by photomultiplier. While the influence of this self-emission can be relatively minimized by a stronger laser light, the intensity of self-emission in this study was significant and could not be disregarded, because the intensity of the laser light had to be kept low in order to measure the burnt gas temperature as precisely as possible. As shown in Figure 2, the extent of self-emission was significantly high as compared to the intensity of transmitted light. To overcome this phenomenon, the Bragg cell was employed to measure the levels of transmitted light and emission simultaneously, and soot concentration was measured by

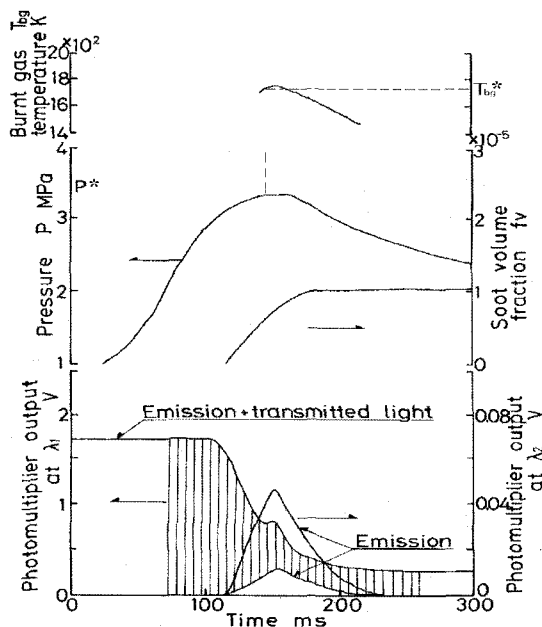


Figure 2. Typical data of emissions, emitted + transmitted light, pressure  $P$ , soot volume fraction  $f_v$  and burnt gas temperature  $T_{bg}$  as a function of time. Conditions: laminar combustion, 8 points ignition, equivalence ratio  $\phi=2.1$  and initial pressure  $P_i=0.89 \text{ MPa}$ .

subtracting self-emission from the total light intensity.

Since the temperatures of soot particles among flames are measured by two-color pyrometry method that focuses on the radiation from soot particles, an attempt must be made to elucidate the relation between the temperatures of soot particles and burnt gas. It has been reported that in case of no surface reaction of soot particles, there was almost no difference in the temperatures of soot particles and ambient burnt gas. And this was almost identical with the case when there was surface reaction in soot particles (Matsui *et al.*, 1983; Li and Wallace, 1995). There are two kinds of temperature measurement methods by two-color pyrometry that detects the intensity of self-emission in two wavelengths respectively; absolute and relative values are obtained by these methods. This study adopted an improved two-color method that was modified from the relative-value measurement (Bae, 1989; Matsui *et al.*, 1983; Bae, 1999). The equation for calculating burnt gas temperature using self-emission intensities  $E_1$  and  $E_2$  is as follows:

$$T_{bg} = \frac{C_2(1/\lambda_2 - 1/\lambda_1)}{\ln[\alpha_1/\alpha_2 \cdot \epsilon_1/\epsilon_2 \cdot E_1/E_2 \cdot (\lambda_1/\lambda_2)^5]} \quad (3)$$

where  $C_2$  refers to a constant for secondary radiation ( $1.438 \text{ cm}\cdot\text{K}$ );  $\lambda$ , effective wavelength calibrated by a black body furnace (Matsui *et al.*, 1983);  $\alpha$ , characteristic constant of optical device employed, that is, calibrated values determined by the black body furnace at an emissivity of 0.981;  $\epsilon$ , flame emissivity; and the subscripts 1 and 2 refer to values at effective wavelength  $\lambda_1$  and  $\lambda_2$  respectively.

Figure 2 shows a set of typical time records of measured values and analyzed results when equivalence ratio  $\phi=2.1$ , initial pressure  $P_i=0.89 \text{ MPa}$  and argon volume fraction in the inert gases  $Ar/(Ar+N_2)=0$ . In the lower part of the figure are raw data of transmitted light and self-emission intensities developed; in the middle are pressure  $P$  measured by a pressure transducer and soot volume fraction  $f_v$ ; and in the higher part is the measured values of burnt gas temperature  $T_{bg}$ . As shown in the figure, soot is formed around the maximum pressure point. It is well documented that soot formation is affected by the temporal variation in temperature and pressure, and as is noticed in the figure, burnt gas temperature  $T_{bg}$  and pressure  $P$  both varied during soot formation. As representative values of pressure and temperature during soot formation, therefore, this study used those values that were measured when soot volume fraction  $f_v$  reached at a half of the final soot volume fraction  $f_v^*$ ; these two resultant values were represented as  $P^*$  and  $T_{bg}^*$ .  $P^*$  can be varied by changing the initial pressure of mixtures. While  $T_{bg}^*$  can doubtlessly vary with the initial pressure, it also can be varied by changing the volume fraction of nitrogen or argon in inert gases. In

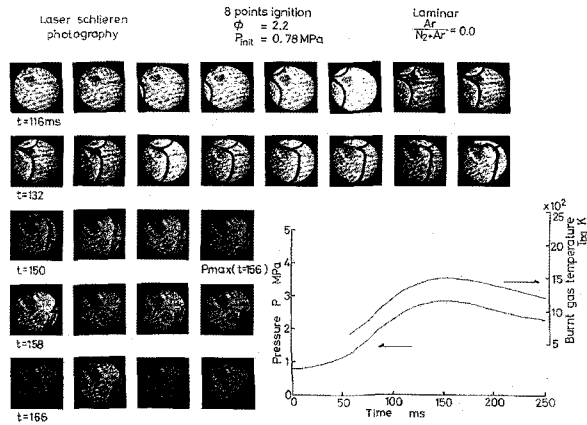


Figure 3. High-speed laser schlieren photographs in observed region. Conditions: laminar combustion, eight-point ignition, equivalence ratio  $\phi=2.2$ , initial pressure  $P_i=0.78$  MPa and  $Ar/(Ar+N_2)=0$ .

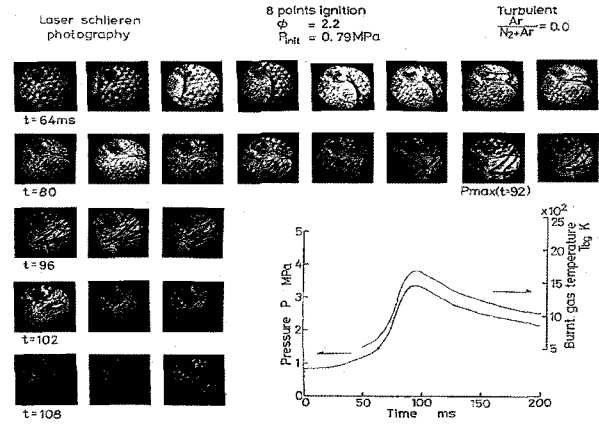


Figure 5. High-speed laser schlieren photographs in observed region. Conditions: turbulent combustion, eight-point ignition, equivalence ratio  $\phi=2.2$ , initial pressure  $P_i=0.79$  MPa and  $Ar/(Ar+N_2)=0$ .

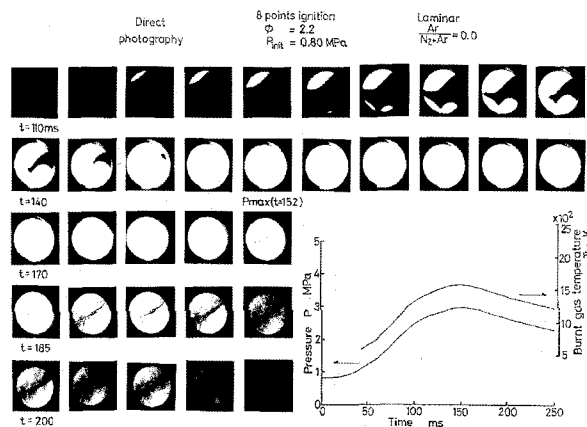


Figure 4. Direct photographs in observed region. Conditions: laminar combustion, eight-point ignition, equivalence ratio  $\phi=2.2$ , initial pressure  $P_i=0.80$  MPa and  $Ar/(Ar + N_2) = 0$ .

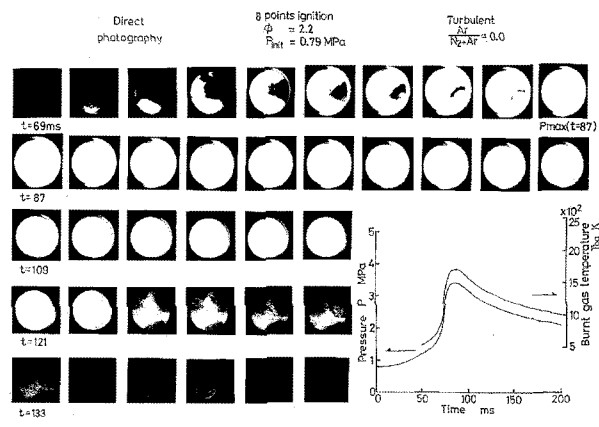


Figure 6. Direct photographs in observed region. Conditions: turbulent combustion, eight-point ignition, equivalence ratio  $\phi=2.2$ , initial pressure  $P_i=0.79$  MPa and  $Ar/(Ar+N_2)=0$ .

this study, soot yield  $C_s^*$  was calculated based on the final value of  $f_v$  in the figure, and the final value of  $f_v$  was calculated as an average value of measurements taken during the 50 ms after combustion was completed and thus soot volume fraction  $f_v$  came to a plateau value.

### 3. RESULTS AND DISCUSSION

#### 3.1. Behavior of Burnt Gas in the Observation Area

In order to make a qualitative observation of flame behavior in the combustion chamber, high-speed laser schlieren and direct photographs were taken of the 10 mm observation area at the center of the constant-volume combustor. For laser schlieren photographing, He-Ne laser beam (wavelength=632.8 nm and output power 1 mW) was enlarged by two convex lenses, before passing

through the observation window in the combustor, and it was directed through a band-pass filter with central wavelength of 635.1 nm (FWHM 3 nm) before traveling into a high-speed camera (HYCAM II). For direct photographing, a mirror was installed in a way that self-emission only would be collected from the flames. The high-speed camera was set at 1000 and 2000 frames per second, at the shutter constant of 1/2.5 and at the iris of 3.5. As a way of synchronizing combustion pressure with photographing, a simple electric circuit device was manufactured and connected to the ignition device so as to record timing and event marks of combustion pressure using the marking generator.

Photos were taken under 24 conditions to investigate the effects of burnt gas temperature and initial pressure at soot-forming equivalence ratio, and the photographing at

the same condition was repeated two or three times for examining the reproductibility and reconfirmation according to circumstances. Figures 3, 4, 5, and 6 show laser schlieren and direct photographs taken of laminar and turbulent combustions under equivalence ratio  $\phi=2.2$ , initial pressure  $P_i=0.78-0.80$  MPa and argon volume fraction in the inert gases  $Ar/(N_2+Ar)=0$ . For the measurement of turbulent combustion, a turbulence generator (hole area ratio to the total area, 15.4%) with an inner diameter of 50 mm, a height of 14 mm, a thickness of 2 mm and 27 holes (4 mm in diameter) was manufactured and put into the center of the combustion chamber. Turbulent flames were generated when laminar flames propagated from the eight spark ignition plugs were passed through this porous cylinder (Bae, 2001).

The examined results of flame behavior based on the two sets of high-speed photographs showed that in the case of laminar combustion, the flames in the observation area had a clear-cut line separating into burnt and unburnt gases; that the flame front didn't fall into disorder; and that the flames converged into the center of the combustion chamber. Though not presented in this paper, the flame front progressed toward the center regardless of the initial pressure and the volume fraction of argon in the inert gases. This meant that in the case of laminar combustion, the gases in the observation area made almost no movement at all regardless of the argon volume fraction in the inert gases and initial pressure. Even though previous study (Bae and Kamimoto, 1995) found that when the eight spark plugs were ignited simultaneously, ignited flames at each of the position were propagated into the central area while the flame front was made round, this study found that there existed some flames that arrived at the 10 mm observation area of the center earlier than others among eight flames.

While flame fronts are also observable in turbulent combustion, they are not as obvious as compared with laminar combustion because of turbulence and fast speed of flames. In addition, turbulent flames tend to contain a considerable amount of unburnt gas, because rapid flame transmission speed (Hamamoto *et al.*, 1987) and turbulence cause irregular shapes in the flame fronts and flames from the eight ignition plugs are mixed. That is to say, turbulence showed significantly greater gas movement.

3.2. Effect of Combustion Pressure and Temperature on Soot Yield  $C_s^*$

The greater pressure  $P^*$  during soot formation is, the greater the final soot volume fraction  $f_v^*$  because of the higher density of initial charged premixture. For a qualitative survey of soot formation, Figure 7 presents soot yield  $C_s^*$  relative to pressure  $P^*$  at equivalence ratio  $\phi=2.1$ , where L and T represent laminar and turbulent

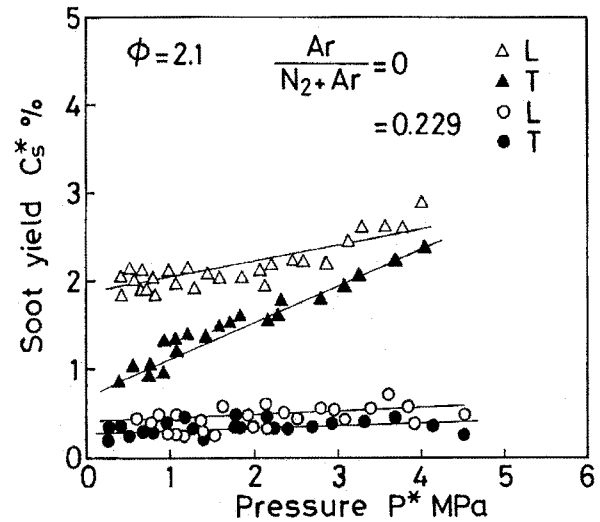


Figure 7. Comparison of soot yield  $C_s^*$  versus pressure  $P^*$  between laminar and turbulent combustion at  $\phi=2.1$ .

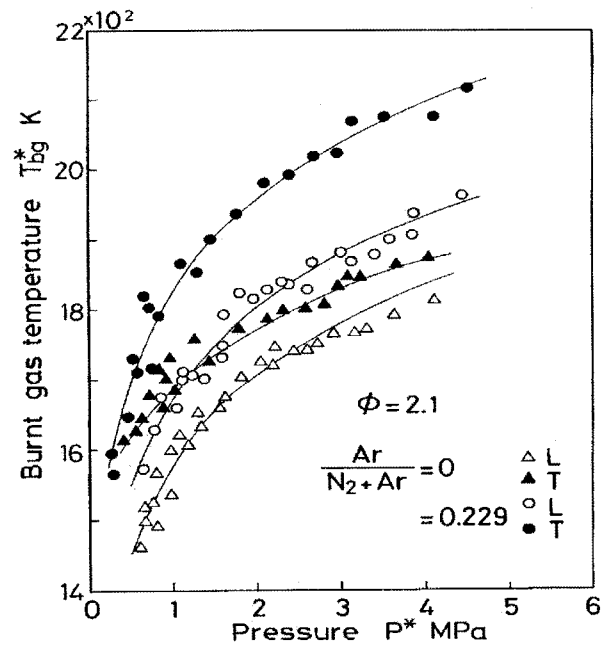


Figure 8. Comparison of burnt gas temperature  $T_{bg}^*$  versus pressure  $P^*$  between laminar and turbulent combustion at  $\phi=2.1$ .

combustions respectively. As shown in the figure,  $C_s^*$  increased with  $P^*$  when equivalence ratio was constant. This tendency was similar to the results of burner premixed flame (MacFarlane *et al.*, 1964; Mätzing and Wagner, 1986) and constant-volume premixed flames (Kamimoto *et al.*, 1989). A major problem with Figure 7 is that it probably contains not only the effect of pressure but also that of temperature. Figure 8 shows the relation

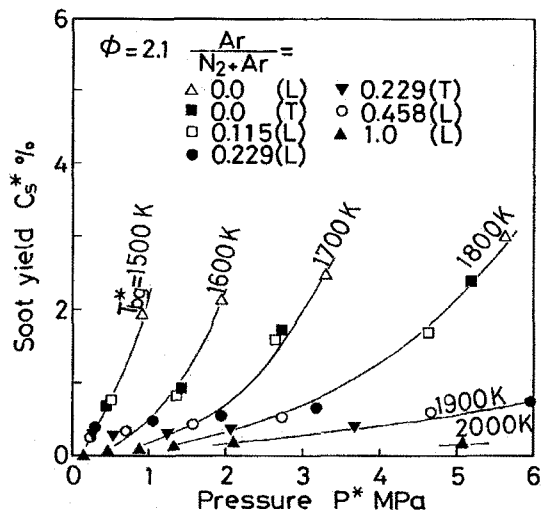


Figure 9. Correlation between soot yield  $C_s^*$  and pressure  $P^*$  for laminar and turbulent combustion as a parameter of burnt gas temperature  $T_{bg}^*$  at  $\phi = 2.1$ .

between  $T_{bg}^*$  and  $P^*$  for each of the data in Figure 7.

In Figure 8, higher pressure caused decrease in heat loss rate of burnt gas per unit mass, thereby resulting in higher  $T_{bg}^*$ . That is, the effects of pressure and temperature are combined in the data of Figure 7. In order to investigate the effect of temperature alone on soot yield  $C_s^*$ , the argon volume fraction among the constant inert gases ( $N_2+Ar$ ) was varied in premixed gas with fixed equivalence ratio to control the burnt gas temperature. Figures 7 and 8 present the measured data at  $Ar/(N_2+Ar) = 0$  and 0.229;  $T_{bg}^*$  increases as the argon volume fraction is increased because the heat capacity of argon is lower compared to that of nitrogen. This means that the higher is the argon volume fraction, the less is the soot yield  $C_s^*$ . To extract the individual effects of pressure and temperature on  $C_s^*$ , Figure 9 shows the relation between  $C_s^*$  and  $P^*$ , with  $T_{bg}^*$  as a parameter. In Figure 9, other data are included in addition to data obtained from  $Ar/(N_2 + Ar) = 0$  and 0.229 at equivalence ratio  $\phi = 2.1$ ; as noticed in the figure, at lower temperatures,  $C_s^*$  drastically increased with pressure, while  $C_s^*$  decreased as the temperature increased, resulting in weaker effect of pressure. In addition, when  $P^*$  was constant, soot yield  $C_s^*$  decreased with  $T_{bg}^*$ .

This tendency was also observed in previous experiments with the shock tube using fuel-inert mixture (Bae, 1989), because higher temperature promoted faster fragmentation process, which delayed the reaction of soot formation from the products of pyrolysis. In experiments with premixed flames, the reason may be attributed to the possibility that the oxidation of soot may be encouraged by  $O_2$  and  $OH$  as the flame temperature is sufficiently high (Köylü *et al.*, 1997).

### 3.3. The Effect of Turbulent Combustion on Soot Yield $C_s^*$

A question that can be raised with the experimental apparatus used in this study is that the low temperature in the vicinity of the inner wall of the combustor may increase the soot formation. It may be expected that turbulent combustion will produce thinner temperature boundary layers. In order to investigate the effect of temperature boundary layers on soot formation, soot yield in turbulent combustion was measured to compare with the result obtained in laminar combustion.

At equivalence ratio  $\phi = 2.1$  and at  $Ar/(N_2+Ar) = 0$  and 0.229, the relation between pressure  $P^*$  and  $T_{bg}^*$  in laminar and turbulent combustions is presented in Figure 8, and the relation between the corresponding  $P^*$  to Figure 8 and soot yield  $C_s^*$  is shown in Figure 7. Burnt gas temperature  $T_{bg}^*$  in turbulent combustion increased by 50 to 150 K due to decrease in combustion duration as compared to laminar combustion, resulting in the corresponding decrease in  $C_s^*$ . Figure 9 offers an overview of the results. Measurements on both turbulent and laminar combustion can be plotted almost on the same curves if  $T_{bg}^*$  for both laminar and turbulent combustion are identical, which means that the effect of temperature boundary layers on soot formation is negligible.

## 4. CONCLUSIONS

An experimental study was performed to investigate independently the effects of pressure and temperature on soot formation of the turbulent and laminar combustions for a premixed propane-oxygen-inert gas flame in a constant-volume combustor. The findings are as follow:

- (1) Measurements of temporal variation in soot formation process at high pressures were possible because pre-mixture in the observation area underwent constant-pressure combustion in the constant-volume combustor during the final stage of combustion at the highest pressure and because the gases of the observation area in the laminar combustion made almost no movement.
- (2) At a constant equivalence ratio, soot yield increased with dropping the temperature and raising the pressure.
- (3) Soot yield was smaller in turbulent than in laminar combustions, because the reduction of heat loss in the former combustion resulted in higher burnt gas temperature.

**ACKNOWLEDGEMENT**—This study was performed in an international collaborative research with Professor Emeritus T. Kamimoto at Tokyo Institute of Technology, financially supported by a Short-term Visit Program of the Japanese Rotary Yoneyama Memorial Foundation, the Basic Research Program of the Korea Science & Engineering Foundation (Grant No.

R01-2000-0000-00307-0), the Research Center for Aircraft Parts Technology of Gyeongsang National University, the 2nd stage Brain Korea 21 Project and NURI. We would like to thank all the people involved in this project.

## REFERENCES

- Bae, M. W. (1989). *A Study on Soot Formation in Premixed Combustion at High Pressures*. Ph. D. Dissertation. Tokyo Institute of Technology, 1–168. Japan.
- Bae, M. W. (1999). A study on the measurement of burnt gas temperature in premixed combustion by modified two-color method. *Trans. Korean Society of Automotive Engineers* **7**, **8**, 43–54.
- Bae, M. W. (2001). A study on soot formation of turbulent premixed propane flames in a constant-volume combustor at high temperatures and high pressures. *Trans. Korean Society of Automotive Engineers* **9**, **4**, 1–9.
- Bae, M. W. and Kamimoto, T. (1995). Soot formation rate in premixed combustion at high pressures. *High-Speed Photography and Photonics, Int. Society for Optical Engineering* **2513**, **1**, 463–471.
- Dalzell, W. H. and Sarofim, A. F. (1969). Optical constants of soot and their application to heat flux calculations. *Trans. ASME, J. Heat Transfer*, **91**, 100–104.
- Hamamoto, Y., Tomita, E. and Izumi, M. (1987). The effect of swirl on the combustion of a homogeneous mixture in a closed vessel. *Trans. JSME(B)* **53**, **488**, 1395–1402.
- Kamimoto, T., Bae, M. W. and Kobayashi, H. (1989). A study on soot formation in premixed constant-volume propane combustion. *Combustion and Flame*, **75**, 221–228.
- Kazakov, A. and Frenklach, M. (1998). Dynamic modeling of soot particle coagulation and aggregation: Implementation with the method of moments and application to high-pressure laminar premixed flames. *Combustion and Flame*, **114**, 484–501.
- Kennedy, I. M. (1997). Models of soot formation and oxidation. *Prog. Energy Combustion Sci.*, **23**, 95–132.
- Kim, H., Lee, S., Kim, J., Cho, G., Sung, N. and Jeong, Y. (2005). Measurement of size distribution of diesel particles: Effects of instruments, dilution methods, and measuring positions. *Int. J. Automotive Technology* **6**, **2**, 119–124.
- Köylü, Ü. Ö., Mcenally, C. S., Rosner, D. E. and Pfefferle, L. D. (1997). Simultaneous measurements of soot volume fraction and particle size/microstructure in flames using a thermophoretic sampling technique. *Combustion and Flame*, **110**, 494–507.
- Li, X. and Wallace, J. S. (1995). In-cylinder measurement of temperature and soot concentration using the two-color method. *SAE Paper No. 950848*, 147–157.
- MacFarlane, J. J., Holderness, F. H. and Witcher, F. S. (1964). Soot formation rates in premixed C5- and C6-Hydro-carbon air flames at pressures up to 20 atmospheres. *Combustion and Flame*, **8**, 215–229.
- Matsui, H., Kamimoto T. and Matsuoka, S. (1983). Formation and oxidation processes of soot particulate in a D. I. diesel engine - An experimental study via the two-color method. *SAE Paper No. 820464*, 1923–1935.
- Mätzing, H. and Wagner, H. G. (1986). Measurements about the influence of pressure on carbon formation in premixed laminar C<sub>2</sub>H<sub>4</sub>-air flames. *21st Symp. (Int.) Combustion, The Combustion Institute*, 1047–1055.
- Park, C. and Appleton, J. P. (1973). Shock-tube measurements of soot oxidation rates. *Combustion and Flame*, **20**, 369–379.